DESIGN AND MODEL SIMULATIONS OF INVERSE CERENKOV ACCELERATION USING INVERSE FREE ELECTRON LASER PREBUNCHING

W. D. Kimura,[*] M. Babzien,[†] I. Ben-Zvi,[†] D. B. Cline,[‡] R. B. Fiorito,[‡‡] J. R. Fontana,[§] J. C. Gallardo,[†] S. C. Gottschalk,[*] P. He,[‡] K. P. Kusche,[*†] Y. Liu,[‡] R. H. Pantell,[**] I. V. Pogorelsky,[†] D. C. Quimby,[*] K. E. Robinson,[*] D. W. Rule,[‡‡] J. Sandweiss,[††] J. Skaritka,[†] A. van Steenbergen,[†] and V. Yakimenko.[†]

[*]STI Optronics, Inc.; [†]Brookhaven National Laboratory; [‡]University of California at Los Angeles; [§]University of California at Santa Barbara; [**]Stanford University; [††]Yale University; [‡‡]Naval Surface Warfare Center

Abstract

An experiment to use an inverse free electron laser (IFEL) to prebunch at optical wavelengths the electrons entering into an inverse Cerenkov accelerator (ICA) is being prepared at the BNL Accelerator Test Facility (ATF). The design and simulations for this experiment are presented. Microbunches on the order of 2 microns in length separated by 10.6 microns are predicted. Under the anticipated ATF conditions, space charge effects should not be an issue. Minimizing bunch smearing is an important design issue also discussed.

1 BACKGROUND

1.1 Inverse Cerenkov Acceleration (ICA)

Inverse Cerenkov acceleration (ICA) [1] uses a gas (e.g., H_2) to slow the phase velocity of the laser light to enable matching the electron velocity. Phase matching is satisfied when the laser light intersects the *e*-beam at the Cerenkov angle θ_c, where $\theta_c = \cos^{-1}(1/n\beta)$, n is the refractive index of gas and β is the electron velocity divided by c.

The present ICA experiment is located at the BNL Accelerator Test Facility (ATF) where acceleration has been routinely observed since the experiment's first operation in 1995 [2]. It features an axicon-focused, radially-polarized laser beam geometry developed by Fontana and Pantell [3] as depicted in Fig. 1.

1.2 Inverse Free Electron Laser (IFEL)

The inverse free electron laser (IFEL) at BNL [4] uses an 47-cm long electromagnet wiggler to provide phase-matching with the laser light. The laser light travels through a circular sapphire waveguide down the center of the wiggler as depicted in Fig. 2. Note, the BNL IFEL wiggler has been designed for easy modification if necessary.

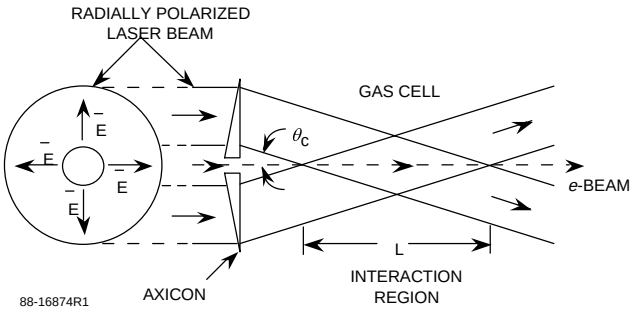

Figure 1: Schematic of basic ICA geometry used in experiment at the ATF [from Ref. 1].

1.3 Motivation for Combining ICA and IFEL Experiments

In the current ICA and IFEL experiments, the 10-ps long electron bunch is much longer than the ~300 ps CO_2 laser pulse. Consequently, electrons intersect the laser light over all phases resulting in both acceleration and deceleration of particles. For efficient acceleration, the electrons must be prebunched into microbunches that are a fraction of the laser wavelength in duration (e.g., for 10.6 μm light, the microbunch length should be ~1-2 μm). These microbunches can then be accelerated as a group by intersecting them at the proper phase with the light wave.

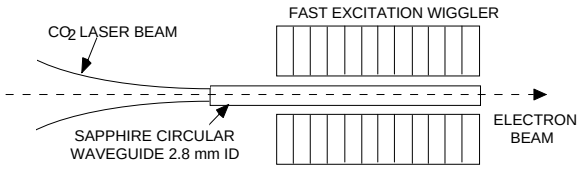

Figure 2: Schematic of basic BNL IFEL geometry.

The present ICA and IFEL experiments modulate the electron energies; thereby, creating these microbunches. An IFEL is a better prebuncher than an ICA device because it does not suffer from scattering of the electrons off the gas molecules. On the other hand, an ICA device scales in energy more favorably than an IFEL

0-7803-4376-X/98/$10.00 © 1998 IEEE

because it does not suffer from synchrotron radiation losses. Gas scattering effects also diminish greatly at high *e*-beam energies.

Hence, the experiments are being combined where the IFEL and ICA devices will be used as a prebuncher and acceleration stage, respectively. The ultimate goal of this combined experiment is to demonstrate 100 MeV of net energy gain.

A conceptual design of the ICA/IFEL experiment is shown in Fig. 3. The drive laser is the ATF CO_2 laser that is capable of delivering 5-10 GW to the gas cell. It is being upgraded to eventually deliver up to 1 TW. The electrons leave the ICA stage where their energies are measured with a spectrometer.

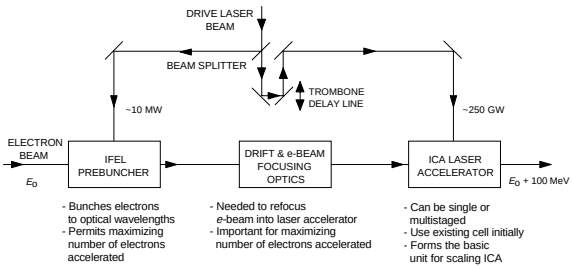

Figure 3: Conceptual design for ICA/IFEL experiment.

2 INTEGRATED MODEL DEVELOPMENT

In order to design and predict the performance of this combined experiment, existing Monte Carlo computer models of the IFEL and ICA were combined into an integrated model. The IFEL model calculates the energy modulation induced on the initial electron distribution. A ray-tracing model of the drift region computes the microbunching resulting from the induced energy spread, including bunch smearing effects due to finite emittance and path length differences through the quadrupole system used for refocusing the beam into the ICA cell (see Fig. 3). The ICA code is used to simulate the acceleration of the prebunched beam in the ICA gas cell, including relevant effects such as laser focusing and electron scattering from the phase matching gas.

2.1 IFEL Design Analysis

Table I lists the IFEL baseline parameters including the typical ATF *e*-beam characteristics entering the IFEL.

IFEL simulations indicate that a uniform 47-cm wiggler with period ≥3.3 cm is suitable over a 40-65 MeV range. The distance between the IFEL and ICA devices is ≈2 m and is constrained by space limitations. To achieve optimum bunching at this distance for a 50 MeV beam requires a modest ~5 MW of laser power to the IFEL. However, the initial energy spread must be much less than the induced energy spread of 1.2%.

The IFEL sensitivity study established other maximum allowable error tolerances: Laser power fluctuations <±50%, energy detuning <±1%, e-beam energy jitter <0.25% p-p, and wiggler current jitter <0.9% p-p.

Table I. IFEL Baseline Parameters

Parameter	Baseline Value
Wiggler	
Length, L_w	47 cm
Period, λ_w	3.33 cm
Peak field, B_o	1.04 T
Wiggler parameter, K	3.23
Energy taper, $\Delta\gamma_r/\gamma_r$	0%
Laser Beam	
Wavelength, λ_L	10.6 μm
Power, P_L	5 MW
Electron Beam	
Energy, E	50 MeV
Energy spread, $\Delta\gamma/\gamma$	0.25% FWHM
Normalized rms emittance	2π mm-mrad
Matched beam Twiss parameters at wiggler exit	β_x = 0.6 m β_y = 0.245 m α_x = -1 α_y = 0

2.2 Drift Region Analysis With Bunch Smearing

Table II lists the drift region baseline parameters. The primary focusing element in this drift region is a triplet consisting of three 20-cm quadrupoles.

Table II. Drift Region Baseline Parameters.

Parameter	Baseline Value
Overall Drift Length, L_D	1.97 m
Separation between quadrupoles	5.2 cm
Distance from end of triplet to ICA cell	38 cm
Magnetic field gradients	25.5 kG/m -45.5 kG/m 34.0 kG/m
Twiss parameters at ICA cell	β_x = 0.065 m β_y = 0.095 m α_x = 0.1 α_y = 0.1
e-Beam diameter at ICA cell (90% of particles)	154 μm × 186 μm

Using these drift region baseline parameters, the effects on bunch smearing as a function of *e*-beam initial energy spread and emittance are shown in Fig. 4.

This indicates that base widths of order 3 μm (implying bunch widths <2 μm FWHM) are obtainable for initial energy spread ≤ 0.25% and emittance ≤ 2π mm-mrad, which are values obtainable on the ATF.

2.3 ICA Performance Prediction

The microbunched beam is lastly sent through the ICA model whose baseline parameters are listed in Table III.

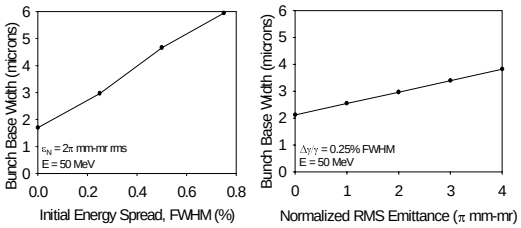

Figure 4. Microbunch base width vs. initial energy spread and emittance.

Table III. ICA Baseline Parameters.

Parameter	Baseline Value
Cerenkov angle, θ_c	20 mrad
Interaction length, L	20 cm
Hydrogen gas pressure, P	1.9 atm
E-beam window thickness	2.1 μm (diamond)

The predictions of the baseline integrated model for a 600 GW laser beam delivered to the ICA gas cell are given in Fig. 5.

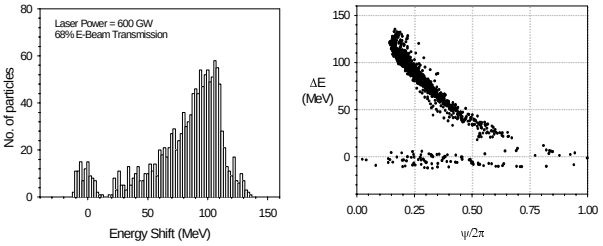

Figure 5. Model prediction of electron energy and phase-space for 600 GW laser beam driving ICA cell.

Notice that a significant number of the 50-MeV electrons have been trapped and accelerated around the 100 MeV point. From the phase diagram it is clear the electron energy spread is caused by particles distributed over phase. Sending these electrons through additional acceleration stages should help reduce this phase spread, thereby narrowing the energy spread.

3 OTHER DESIGN ISSUES

3.1 Space-Charge Effects

Space-charge effects will become a more serious issue at these extraordinarily small microbunch dimensions. Earlier PARMELA simulations [5] indicate that space-charge effects will tend to broaden the microbunch size by ~10% for the ATF conditions. Further PARMELA analysis is being performed to more fully understand when space-charge effects become significant.

3.2 Measurement of Microbunch Characteristics

Conventional diagnostics cannot measure the bunch length of the 2-μm microbunches. We have been examining using coherent transition radiation (CTR) as a means for detecting the degree of microbunching. Recent CTR experiments at the ATF have successfully detected the IFEL-generated microbunches [6]. We are also examining a novel modification of the basic CTR device that may permit a more direct estimation of the bunch length.

4 CURRENT STATUS AND FUTURE PLANS

As of May 1997, the ICA experiment has been moved downstream from its original location to make room for the IFEL and triplet. We are awaiting delivery of the quadrupoles before finishing the installation of the IFEL during the autumn of 1997.

First experiments will be to test the IFEL and prebunching only. Next the combined ICA/IFEL system will be run at relatively low laser power (e.g., 5 GW). The primary goal of these tests will be to demonstrate rephasing of the laser light with the microbunches and subsequent acceleration. Later much higher laser peak power (e.g., ~300-600 GW) will be delivered to the ICA cell to achieve the amount of acceleration predicted in Fig. 5. Issues such as possible laser damage of the gas cell optics must be addressed at these high laser powers.

5 CONCLUSIONS

The combined ICA/IFEL experiment will be one of the first to demonstrate acceleration of laser-generated microbunched electrons. It will examine issues of microbunch preservation and rephasing with the laser light. It will also address engineering issues related to accelerating fsec-long bunches.

6 ACKNOWLEDGEMENTS

This work was supported by the U.S. Department of Energy, Grant Nos. DE-FG06-93IR40803, DE-AC02-76CH00016, DE-FG03-92ER40695, and DE-FG03-90ER40545.

REFERENCES

[1] J. A. Edighoffer, W. D. Kimura, R. H. Pantell, M. A. Piestrup, and D. Y. Wang, "Observation of Inverse Cerenkov Interaction Between Free Electrons and Laser Light," Phys. Rev. A **23**, 1848-1854, (1981).

[2] W. D. Kimura, G. H. Kim, R. D. Romea, L. C. Steinhauer, I. V. Pogorelsky, K. P. Kusche, R. C. Fernow, X. Wang, and Y. Liu, "Laser Acceleration of Relativistic Electrons Using the Inverse Cerenkov Effect," Phys. Rev. Lett. **74**, 546-549 (1995).

[3] J. R. Fontana and R. H. Pantell, "A High-Energy, Laser Accelerator for Electrons Using the Inverse Cherenkov Effect," J. Appl. Phys. **54**, 4285 (1983).

[4] A. van Steenbergen, J. Gallardo, J. Sandweiss, J-M. Fang, M. Babzien, X. Qiu, J. Skaritka, and X.J. Wang, "Observation of Energy Gain at the BNL Inverse Free-Electron-Laser Accelerator," Phys. Rev. Lett. **77**, 2690 (1996).

[5] A. Bogacz, FNAL, private communication.

[6] Y. Liu, D. B. Cline, X. J. Wang, M. Babzien, J. M Fang, and K. P. Kusche, (in these proceedings).